Food Sci Biotechnol
https://doi.org/10.1007/s10068-017-0193-0

Fabrication of an electrochemical biosensor with ZnO nanoflakes interface for methylglyoxal quantification in food samples

Amudha Jayaprakasan[1,2] · Amarnath Thangavel[1,2] · Lakshmishri Ramachandra Bhat[1,3] · Manju Bhargavi Gumpu[1,3] · Noel Nesakumar[1,3] · K. Jayanth Babu[1,2] · Srinivasan Vedantham[1,2] · John Bosco Balaguru Rayappan[1,3]

Received: 25 April 2017 / Revised: 3 August 2017 / Accepted: 30 August 2017

Abstract Increased consumption of fried foods such as grilled chicken contains elevated levels of methylglyoxal (MG), which is associated with diabetes mellitus. Hence, in this work, glyoxalase 1(GLO 1) based, zinc oxide (ZnO) flakes interfaced mediator free electrochemical biosensor was developed to detect MG in grilled chicken. ZnO flakes were synthesized by direct precipitation method. X-ray diffractometer and field emission scanning electron microscope were used to study the structural and morphological characteristics of ZnO flakes. The immobilization of GLO 1 on Pt/ZnO flakes modified electrode was confirmed by Fourier transform infrared spectroscopy. Cyclic voltammetric and amperometric studies were carried out using Pt/ZnO flakes/GLO 1 working electrode. The developed biosensor exhibited linear range of 0.6–2.0 μM, sensitivity of 0.281 μA μM^{-1}, LOD of 9 nM with a response time of <4 s and shelf life of 18 days (89%).

Keywords Biosensor · ZnO flakes · Human glyoxalase 1 · Methylglyoxal · Cyclic voltammetry · Amperometry

Introduction

Methylglyoxal (MG), an advanced glycation end product is found in food items [1], prepared by frying, grilling, roasting [2, 3] at temperatures above 120 °C [4], dry heat cooking [5], animal fats and bakery products [3]. The estimated mean dietary exposure to MG for adults was 1.3 mg/kg bodyweight/day, and the estimated exposure for high consumers was 3.9 mg/kg bodyweight/day. Similarly, the estimated mean dietary exposure to MG for toddlers was 7.7 mg/kg bodyweight/day, and the estimated exposure for high consumers was 22.8 mg/kg bodyweight/day [2].

The abnormal concentration of MG in human blood is related to diabetes mellitus type 1 (7–8.4 μM), and type 2 (2.8–4.2 μM) [3, 5, 6]. The World Health Organization (WHO) states that the unhealthy eating habit is the major cause for non-communicable diseases like diabetes [7]. In 2012, WHO estimated 200 million diabetics around the world in which 50 million diabetics are Indians [8, 9]. Moreover, the higher concentration of MG will also contribute to the pathophysiology of cardiovascular disease, oxidative stress [6], aging [1], atherosclerosis [5, 10], hypertension [1], chronic kidney diseases, insulin resistance [5] and inflammation [11]. In 2012, Federation Dentaire Internationale stated that "Diabetes and cardiovascular disease are now the leading causes of disease burden and death worldwide" [12].

In the past, the expensive and time consuming complex procedures like gas chromatography–mass spectrometry and high-performance liquid chromatography [13] were

Amudha Jayaprakasan and Amarnath Thangavel have contributed equally to this article.

Electronic supplementary material The online version of this article (doi:10.1007/s10068-017-0193-0) contains supplementary material, which is available to authorized users.

✉ John Bosco Balaguru Rayappan
rjbosco@ece.sastra.edu

[1] Centre for Nanotechnology & Advanced Biomaterials (CeNTAB), SASTRA University, Thanjavur, Tamil Nadu 613 401, India

[2] School of Chemical & Biotechnology, SASTRA University, Thanjavur, Tamil Nadu 613 401, India

[3] School of Electrical & Electronics Engineering, SASTRA University, Thanjavur, Tamil Nadu 613 401, India

Published online: 02 December 2017

developed to detect MG in food products. Recently, non-enzymatic MG electrochemical biosensors were developed by using single walled carbon nanotubes (SWCNTs) and platinum (Pt) nanoparticles [14, 15]. However, specificity and precision were less in these types of electrochemical biosensors. Whereas, in the case of enzyme-based electrochemical biosensors [13, 16–21], high specificity, accuracy and rapidness can be achieved. They were used extensively to detect biological molecules and toxins in clinical diagnosis, food products and in the environment. A similar system was developed using the ionic conductor cerium oxide (CeO_2) [21] which has higher sensitivity but lack the capability to overcome potential interferents and respond rapidly. Thus, in this work, a specific and accurate method for the measurement of MG was considered using glyoxalase 1 (GLO 1) based electrochemical biosensor. In addition, GLO 1 enzyme was added along with the nano-interface to increase the sensitivity and electron transfer rate of the biosensor to the maximum extent. The GLO 1 enzyme reacted with MG and resulted in S-D-Lactoylglutathione [22] production.

$$Methylglyoxal + GSH \rightleftharpoons Hemithioacetal \overset{GLO1}{\rightarrow} S-D-Lactoylglutathione$$

In the recent past, ZnO nanostructures have attracted many researchers [23–27] towards sensing applications due to its merits like fast electron transfer, single molecule detection, high enzyme immobilization efficiency, larger specific surface area and biocompatibility [28–31]. The high-isoelectric point (IEP = 9.5) of ZnO nanoparticles facilitates the immobilization of low-isoelectric point (IEP = 5.9) GLO 1 enzyme through electrostatic interactions [32].

Different morphology of ZnO nanoparticles used for enzyme immobilization in electrochemical biosensors show diverse analytical response characteristics. For example, Ali et al. [33] studied the uric acid detection response of shape specific ZnO nanoparticles based electrochemical biosensor. They compared the sensitivity of modified bio-electrode based on ZnO nanowire (sensitivity = 29 mV/decade) with ZnO flakes in which ZnO flakes interfaced biosensor showed more than 2-fold higher sensitivity (66 mV/decade). In this study, ZnO flakes with unique properties such as rough and large surface area were prepared. ZnO flakes also offered a higher surface to volume ratio that provided a favourable microenvironment for the immobilization of the GLO 1, which in-turn increased the sensitivity and the stability of the biosensor [34, 35].

In this work, a simple direct precipitation method [29] was used to prepare ZnO flakes. This method has many advantages like relatively low temperature for synthesis, cost effective, scalable, less time consuming, repeatable and easy to control over the other methods like solvothermal method, hydrothermal method, chemical vapour deposition, and physical vapour deposition. These methods require multiple steps, sophisticated equipment, high temperature and high pressure. In addition, the applicability of the ZnO flakes as a MG biosensor by immobilizing GLO 1 enzyme on the ZnO flakes surface was examined and the fabricated bio-electrode was used to detect MG in grilled chicken samples.

Materials and methods

Materials and reagents

Hydroxylammonium hydrochloride ($NH_2OH.HCl$) was purchased from Chemspure, India. Zinc nitrate hexahydrate ($Zn(NO_3)_2.6H_2O$) was purchased from S D Fine-Chem Limited, India. Glyoxalase 1 [Human, Molecular weight: 20.7 kDa, ≥90% (SDS-PAGE)] and methylglyoxal (Molecular weight: 69.49 g M^{-1}) were procured from Sigma-Aldrich, USA. L-Glutathione-reduced (Molecular weight: 307.32 g M^{-1}) was purchased from Hi-Media, India. Other chemicals like sodium hydroxide, chitosan, ascorbic acid, glucose, urea, lactic acid, monobasic sodium phosphate and dibasic sodium phosphate were purchased from Merck India Ltd., India. Nickel acetate, zinc acetate and cupric acetate were purchased from Thermo Fisher Scientific Pvt. Ltd., India. The working electrode Pt (2 mm dia, CHI 102), Ag/AgCl reference electrode (CHI 111, 0.5 mm dia) and Pt wire counter electrode (CHI 115, 0.5 mm dia) were purchased from CH Instruments, Inc., USA. All the reagents and solutions were prepared using doubly de-ionized water (Aqua purification systems, India).

ZnO flakes synthesis

ZnO flakes were synthesized by direct precipitation method [36] at pH 10. Zinc nitrate hexahydrate of 5.6 g (0.3 M), 0.69 g of hydroxylammonium hydrochloride (0.1 M) and 1.19 g of sodium hydroxide (0.3 M NaOH) were dissolved in 100 mL of distilled water and stirred for 30 min. Then 100 mL (1 M) solution of NaOH was prepared and added drop-wise to the precursor solution to get pH 10 with constant stirring at room temperature. This solution was further heated at 60 °C for 20 min. Then the solution was filtered and the precipitate was washed using methanol many times. The sample was annealed at 525 °C for 5 h.

Fabrication of Pt/ZnO flakes/GLO 1 bio-electrode

Figure 1(A) shows the schematic representation of the proposed Pt/ZnO flakes based MG biosensor. To prepare a

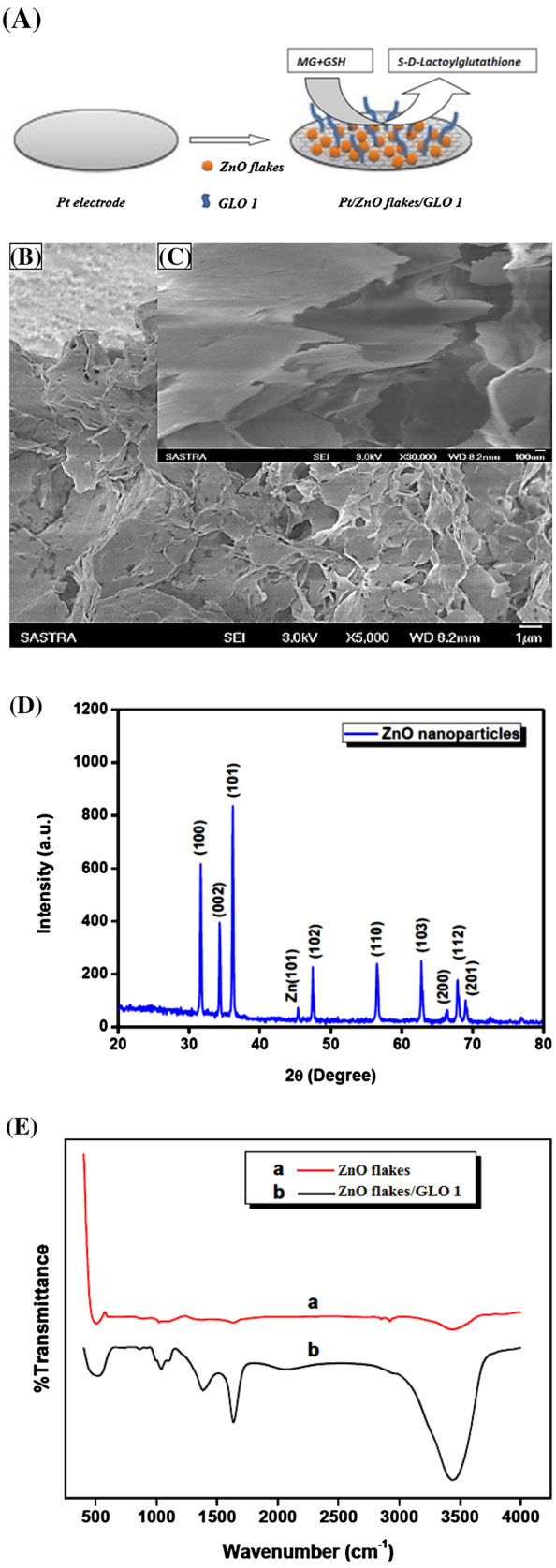

◀**Fig. 1** (**A**) Schematic representation of the proposed Pt/ZnO flakes based MG biosensor. (**B**) typical low- and (**C**) high-magnification FE-SEM images of ZnO flakes and (**D**) XRD pattern of ZnO nanoparticles, (**E**) FT-IR spectra of ZnO flakes in the absence (*a*) and presence (*b*) of GLO 1

bio-electrode using Pt working electrode with ZnO flakes and GLO 1 enzyme, 1 mg of ZnO flakes was weighed by using digital balance (BT 224 s, Sartorius) and it was further added to 100 µL of phosphate buffered saline (0.1 M PBS, 7.4 pH) containing 1 µL of chitosan. This mixture was sonicated for 1 h. To this solution, 10 µL of GLO 1 was added and sonicated for another 2 min to disperse the GLO 1 uniformly. Finally, 3 µL of this product was uniformly added on the Pt working electrode. Thus, the Pt/ZnO flakes/GLO 1 bio-electrode was fabricated.

Characterization techniques

X-ray Diffractometer (XRD) (D8 Focus, Bruker, Germany) was used to study the structural characteristics of ZnO flakes. Field Emission Scanning Electron Microscopy (FE-SEM) (JSM 6701F, JOEL, Japan) was used to observe the surface morphology of ZnO flakes. To study the immobilization of GLO 1 on to ZnO flakes decorated Pt electrode, Fourier transform infrared spectrometer (FT-IR) (Spectrum 100, Perkin Elmer, USA) was used.

Electrochemical measurements

The conventional three electrode system comprising of modified working electrode (Pt/ZnO flakes/GLO 1), Pt as counter electrode, and Ag/AgCl saturated in 0.1 M KCl as reference electrode was employed. All the electrochemical studies were carried out using an electrochemical analyser (CHI 600C, CH Instruments, USA) at room temperature.

Results and discussion

Characterization of ZnO flakes

FE-SEM analysis

Figure 1(B), (C) shows the typical low- and high-magnification FE-SEM images of ZnO flakes. The flakes morphology of ZnO nanoparticles was observed with the mean width and wall thickness of 0.997 ± 0.516 µm (n = 40; RSD = 52.728%) and 44.065 ± 10.882 nm (n = 40; RSD = 24.697%) respectively [39]. The high RSD values observed in the mean width and wall thickness of ZnO flakes showed that the ZnO flakes were poly-dispersed. It

also indicated the high surface roughness of the ZnO flakes, which in-turn favoured the immobilization of the enzyme GLO 1 on their surface.

X-ray diffraction analysis

Figure 1(D) shows the XRD pattern of ZnO flakes synthesized by direct precipitation method. The ZnO exhibited hexagonal wurtzite structure with polycrystalline nature which was confirmed by the characteristic diffraction peaks positioned at 2θ values of 31.66°, 34.33°, 36.15°, 47.46°, 56.51°, 62.78°, 66.30°, 67.86°, 69.02° and 76.87° were correspond to (100), (002), (101), (102), (110), (103), (200), (112), and (201) crystal planes respectively. In addition, the diffraction pattern of Zn (101) was also appeared in ZnO flakes. The obtained results were found to be in agreement with the JCPDS Card No. 01-089-7102 [37, 38]. An increase in peak intensity corresponding to (101) crystal plane indicated that the growth of ZnO flakes was preferentially oriented towards (101) crystal plane.

FT-IR analysis

Figure 1(E) shows the FT-IR spectra of ZnO flakes in the absence (a) and presence (b) of GLO 1. Curve (a) shows a peak at 506 cm^{-1} corresponds to Zn–O stretching band which confirmed the formation of ZnO nanoparticles [40]. Curve (b) shows peaks at 1100.96, 1040.01, 1384.01 and 1633.72 cm^{-1} correspond to C–O stretch, aromatic C–H in plane bending, OH bending [41] and β sheets of GLO 1 [42, 43] respectively. The last peak confirmed the immobilization of GLO 1 with ZnO flakes. The peak at 3434.34 cm^{-1} corresponding to the H-bonded OH stretch was found to be increased in the presence of GLO 1 than in the absence of GLO 1 implying the existence of water molecules sticking on the ZnO flakes surface [41, 42].

Electrochemical studies

Effect of ZnO flakes on the electrochemical reaction

Cyclic voltammogram profiles of Pt/ZnO flakes/GLO 1 bio-electrode obtained at a scan rate of 0.2 V s^{-1} for 1 μM MG using modified and unmodified Pt electrodes in PBS (0.1 M, pH 7.4) containing 100 μM GSH are shown in Fig. 2(A). Table 1 shows the electrochemical parameters of various modified electrodes. The bare Pt electrode did not show any peak current (I_p) which revealed the absence of reaction with MG. After the immobilization of GLO 1 on the Pt electrode surface, a cathodic peak current (I_{pc}) was observed indicating the specificity of GLO 1 enzyme towards MG. In the presence of ZnO flakes interface, Pt/ZnO flakes/GLO 1 modified bio-electrode showed a drastic

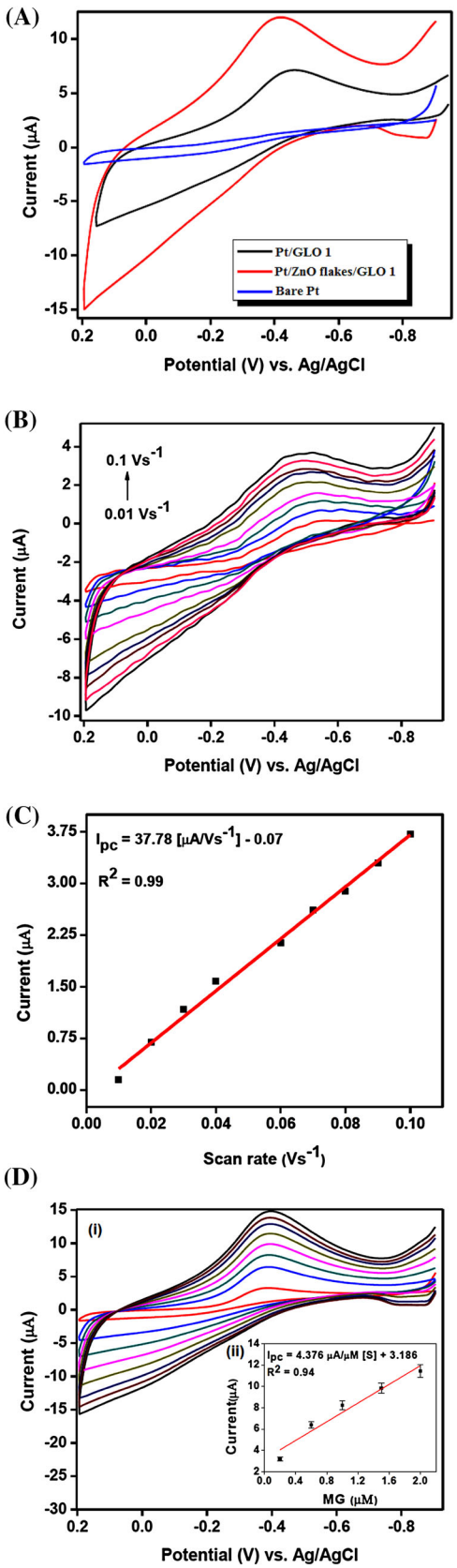

◀**Fig. 2** (**A**) Cyclic voltammogram profiles of Pt/ZnO flakes/GLO 1 bio-electrode obtained at a scan rate of 0.2 V s^{-1} for 1 μM MG using modified and unmodified Pt electrodes in PBS (0.1 M, pH 7.4) containing 100 μM GSH, (**B**) cyclic voltammograms of Pt/ZnO flakes/GLO 1 bio-electrode obtained at different scan rates in the presence of 0.2 μM MG in PBS (0.1 M, 7.4 pH) containing 100 μM GSH, (**C**) Linear dependency of cathodic peak current (I_{pc}) on scan rate (0.01–0.1 V s^{-1}) for Pt/ZnO flakes/GLO 1 bio-electrode and (**D**) cyclic voltammograms of Pt/ZnO flakes/GLO 1 bio-electrode at 0.1 V s^{-1} (*i*) and its linear dependence (*ii*) for varying concentrations of MG (0.2, 0.6, 1.0, 1.5, 2.0, 10, 50 and 100 μM) in PBS (0.1 M, pH 7.4) containing 100 μM GSH

increase in the magnitude of I_{pc} (I_{pc} = 11.97 μA), which was 1.67 times greater than that of Pt/GLO 1 bio-electrode (I_{pc} = 7.137 μA). An increase in current (I_{pc}) might be due to high specific area of ZnO flakes which enhanced the immobilization of GLO 1 and hence, exposed more active sites for MG. The standard reduction potential (E^0) of GSH is −0.230 V (Vs. NHE) and the E^0 for Ag/AgCl reference electrode is 0.222 V [44]. Since the electrochemical studies were done with Ag/AgCl reference electrode, the E^0 got shifted to −0.452 V. Pt/GLO 1 and Pt/ZnO flakes/GLO 1 modified bio-electrodes showed irreversible cyclic voltammetric current with the cathodic peak potential (E_{pc}) of −0.460 and −0.423 V respectively. Moreover, these E_{pc} matched with the E^0 of −0.452 V (Vs. Ag/AgCl) for GSH. This confirmed the reduction reaction of GSH in the cathodic electrochemical process. It also indicated that the GLO 1 enzyme retained its catalytic activity even after the immobilization of GLO 1 on ZnO flakes surface. To study the influence of ZnO flakes in the electrochemical process, full width at half maximum of peak height (FWHM) for Pt/GLO 1 and Pt/ZnO flakes/GLO 1 modified bio-electrodes in PBS (0.1 M, pH 7.4) containing 1 μM MG and 100 μM GSH was compared. In the case of Pt/ZnO flakes/GLO 1 bio-electrode, the FWHM (FWHM = 0.256 V) was approximately 4 mV lesser than that of Pt/GLO 1 bio-electrode (FWHM = 0.260 V) suggesting that the number of electrons shuttled between GLO 1 enzyme and Pt working electrode were more in the presence of ZnO flakes immobilization matrix. Using the electron transfer rate constant formula ($K_s = \frac{I_{pc}}{Q}$, where I_{pc} is the cathodic peak current and Q is the amount of charge consumed), K_s of Pt/GLO 1 and Pt/ZnO flakes/GLO 1 bio-electrodes was calculated. The K_s of Pt/GLO 1 and Pt/ZnO flakes/GLO 1 bio-electrodes was found to be 0.725 and 1.030 s^{-1} respectively showing that the electron transfer between ZnO flakes and GLO 1 enzyme was very rapid in Pt/ZnO flakes/GLO 1 than that of Pt/GLO 1 modified working electrode. The surface coverage ($\Gamma = \frac{Q}{nFA}$, where Q is the amount of charge consumed, F is the Faraday constant, n is the number of electrons transferred and A is the area of Pt working electrode) of MG over Pt/GLO 1 and Pt/ZnO flakes/GLO 1 bio-electrodes was calculated as 0.785 and 0.958 μM cm^{-2} respectively. All these results reconfirmed the improved performance of Pt/ZnO flakes/GLO 1 bio-electrode. Based on the electrochemical analysis, Pt/ZnO flakes/GLO 1 modified bio-electrode was considered for further electrochemical experiments.

Effect of scan rate on Pt/ZnO flakes/GLO 1 bio-electrode

Cyclic voltammograms of Pt/ZnO flakes/GLO 1 bio-electrode obtained at different scan rates in the presence of 0.2 μM MG in PBS (0.1 M, 7.4 pH) containing 100 μM GSH are shown in Fig. 2(B). Linear dependence of cathodic peak current (I_{pc}) on scan rate (0.01–0.1 V s^{-1}) for Pt/ZnO flakes/GLO 1 bio-electrode is shown in Fig. 2(C). For surface controlled electrode reaction, linear dependency of I_{pc} on ν was observed, whereas, for diffusion controlled electrode reaction, linear dependency of I_{pc} on square-root of ν was observed. From 0.01 to 0.1 V s^{-1}, the I_{pc} of Pt/ZnO flakes/GLO 1 bio-electrode was increased linearly with linear regression equation, ($I_{pc} = 37.78[\mu A/Vs^{-1}] - 0.07$) ($R^2 = 0.99$). The linear regression equation was seemed to be in accordance with the surface controlled peak current—surface coverage equation: $I_p = \frac{nFQv}{4RT}$, where n is the number of electrons transferred, R is the rate constant, Q is the amount of charge consumed, F is the Faraday constant, v is the scan rate, T is the absolute temperature and I_p is the peak current. It indicated that the electrochemical reaction occurred in the cathodic process was only due to the surface confined biomolecules. It also showed that by associating GLO 1 with the immobilization matrix of ZnO flakes, it was easy to offer adequate accessibility to electrons to shuttle between GLO 1 and Pt electrode.

Effect of concentration of methylglyoxal

Figure 2(D) shows the cyclic voltammograms of Pt/ZnO flakes/GLO 1 bio-electrode at 0.1 V s^{-1} (i) and its linear dependence (ii) for varying concentrations of MG (0.2, 0.6, 1.0, 1.5, 2.0, 10, 50 and 100 μM) in PBS (0.1 M, pH 7.4)

Table 1 Electrochemical parameters of different modified bio-electrodes

Electrode	I_{pc} (μA)	E_{pc} (V)	FWHM (V)	K_s (s^{-1})	Γ (μM cm^{-2})
Pt/GLO 1	7.137	−0.460	0.260	0.752	0.785
Pt/ZnO flakes/GLO 1	11.970	−0.423	0.256	1.030	0.958

containing 100 μM GSH. The I_{pc} was found to be increased on progressive additions of MG. This MG dependent increase in current response may be ascribed to the increased production of S-D-Lactoylglutathione during the conversion of MG to hemithioacetal by GLO 1 immobilized on Pt/ZnO flakes modified working electrode. Well defined peaks and significant peak to peak separation indicated that the fabrication of Pt/ZnO flakes/GLO 1 bio-electrode and the immobilization of GLO 1 on ZnO flakes surface were not damaged. When the MG concentration increased from 0.2 to 100 μM, there was no shift in E_{pc} ($E_{pc} = -0.423$ V) suggesting that the catalytic activity of GLO 1 enzyme was not affected by the ZnO flakes' interface. As the MG concentration varied from 0.2 to 2.0 μM, the I_{pc} increased in a linear fashion ($I_{pc} = 4.376\,\mu A\,\mu M^{-1}[MG] + 3.186$) with R^2 of 0.96. The sensitivity of the Pt/ZnO flakes/GLO 1 bio-electrode was computed from the calibrated curve and was found to be 4.376 μA μM^{-1}.

Amperometric detection of methylglyoxal using Pt/ZnO flakes/GLO 1 bio-electrode

Figure 3(A) shows the amperogram of Pt/ZnO flakes/GLO 1 bio-electrode at an applied potential of −0.423 V (i) and its linear dependence (ii) for varying concentrations of MG (0.2, 0.6, 1.0, 1.5, 2.0, 10, 30, 50, 70 and 100 μM) in PBS (0.1 M, pH 7.4) containing 100 μM GSH. Owing to the production of S-D-Lactoylglutathione, the value of amperometric current was increased with increase in the concentration of MG. As the MG concentration varied from 0.6 to 2.0 μM, the amperometric current increased in a linear fashion ($I_{pc} = 0.281\,\mu A\,\mu M^{-1}[MG] + 5.097$) with R^2 of 0.96. From the linear curve, the calculated sensitivity was found to be 0.281 μA μM^{-1}. The response time of the developed Pt/ZnO flakes/GLO 1 bio-electrode was found to be less than 4 s. Figure 3(B) shows the nonlinear hyperbolic current response of Pt/ZnO flakes/GLO 1 bio-electrode for varying concentrations of MG. The nonlinear hyperbolic current response of Pt/ZnO flakes/GLO 1 bio-electrode showed that only from 0.6 to 2.0 μM, the amperometric current depended on MG concentration, whereas beyond 2.0 μM, the amperometric current depended on GLO 1 catalytic activity. From 2.0 to 100 μM, the amperometric current seemed curvilinear than linear. This was attributed to the decreased rate of reaction between MG and GLO 1, which in-turn resulted in slow electron transfer between GLO 1 and Pt/ZnO flakes bio-electrode. The maximum current (I_{max}) and Michaelis–Menten constant (K_M) calculated from Lineweaver–Burk equation ($\frac{1}{I_{ss}} = \left(\frac{K_M}{I_{max}}\right)\left(\frac{1}{S}\right) + \left(\frac{1}{I_{max}}\right)$, where I_{ss} is the steady state current, S is the concentration of the MG and I_{max} is

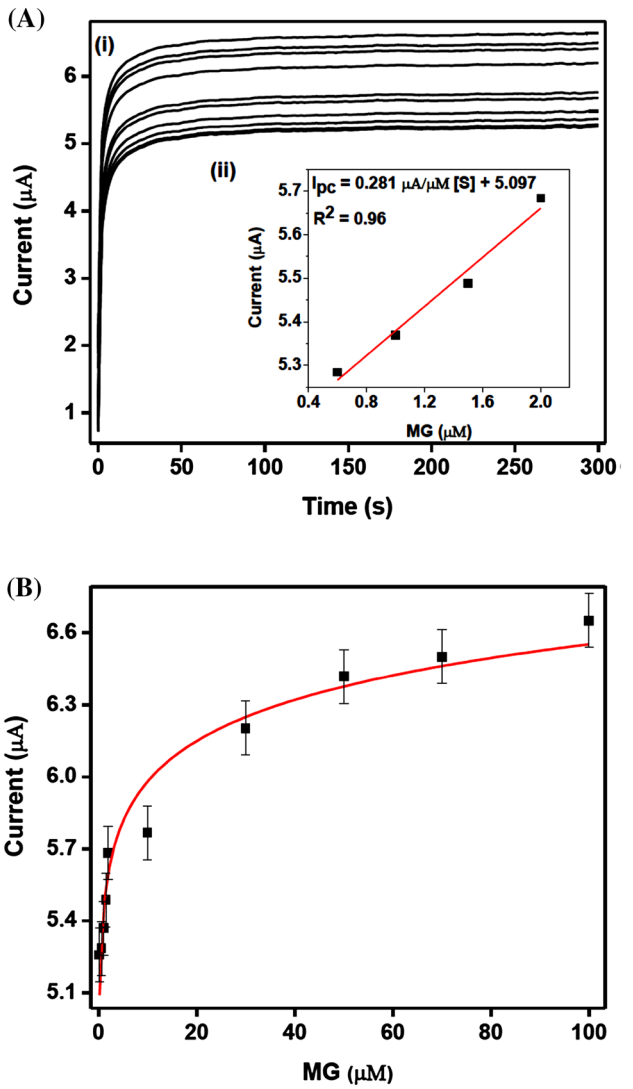

Fig. 3 (**A**) Amperogram of Pt/ZnO flakes/GLO 1 bio-electrode at an applied potential of −0.423 V (*i*) and its linear dependence (*ii*) for varying concentrations of MG (0.2, 0.6, 1.0, 1.5, 2.0, 10, 30, 50, 70 and 100 μM) in PBS (0.1 M, pH 7.4) containing 100 μM GSH and (**B**) Nonlinear hyperbolic current response of Pt/ZnO flakes/GLO 1 bio-electrode for varying concentrations of MG

the maximum current measured under MG saturation) were found to be 6.62 μA and 5.81 μM respectively. The small K_M value indicated that there exists a good affinity between MG and active sites of GLO 1 immobilized on ZnO flakes surface. From the MG dependent dose response analysis, the MG concentration (EC 50) at which Pt/ZnO flakes/GLO 1 modified bio-electrode displaying 50% of amperometric current response was found to be 5.73 μM. Limit of detection ($LOD = 3.3 \times \left(\frac{S_b}{S}\right)$, where S is the sensitivity and S_b is the standard deviation in the absence of MG) and limit of quantification $\left(LOQ = 10 \times \left(\frac{S_b}{S}\right)\right)$ of Pt/ZnO flakes/GLO 1 modified bio-electrode were calculated to be 9 and 27 nM respectively.

Accuracy, precision and biosensor efficiency

Accuracy of Pt/ZnO flakes/GLO 1 modified bio-electrode was computed employing 10, 30 and 70 μM of MG in PBS (0.1 M, pH 7.4) containing 100 μM of GSH. The predicted mean MG concentration ± relative error (n = 3) for 10, 30 and 70 μM of MG were $10 \pm 9 \times 10^{-4}$, $30 \pm 6 \times 10^{-4}$, $70 \pm 3.587 \times 10^{-4}$ μM respectively. These low relative errors showed that the MG biosensor had good accuracy of measurement of MG by Pt/ZnO flakes/GLO 1 bio-electrode. Repeatability and reproducibility of the developed MG biosensor with 0.2 μM of MG in PBS (0.1 M, pH 7.4) containing 100 μM of GSH for intra- (n = 7) and inter-assay (n = 7) were performed and their corresponding RSD% values were statistically analysed. The RSD% value for intra-assay was 1.72 indicating that there was no damage to the modified bio-electrode during repeated usage and the embedding between GLO 1 and Pt/ZnO flakes was good, which in-turn indicated good repeatability of the MG biosensor. The RSD% value for inter-assay was calculated as 2.68 indicating the good reproducibility of the MG biosensor, which in-turn indicated that the fabrication technique of the Pt/ZnO flakes/GLO 1 bio-electrode was good. The biosensor efficiency

$$\left(Biosensorefficiency\% = \frac{I_{max}/K_M}{SlopeofPt/ZnO-NF/GLO1} \times 100\%\right)$$

of Pt/ZnO flakes/GLO 1 bio-electrode was estimated as 405%, suggesting that the immobilized GLO 1 enzyme on ZnO flakes surface can enhance the MG to S-D-Lactoylglutathione conversion in the presence of GSH.

Interference and stability studies

Table S1 shows the degree of inhibition of Pt/ZnO flakes/GLO 1 bio-electrode in the presence of various interferents. The interferences of acetaminophen (0.1 mM), sucrose (0.1 mM), ascorbic acid (0.1 mM), lactic acid (0.1 mM), urea (0.1 mM), Ni^{2+} (0.1 mM), Cd^{2+} (0.1 mM), Zn^{2+} (0.1 mM) and Cu^{2+} (0.1 mM) to the MG response were examined with MG concentration at 0.2 μM. Interference was computed in terms of degree of inhibition or percentage inhibition ($I\% = \left[\frac{I_0 - I_i}{I_0}\right] \times 100$, where I_i and I_0 are the amperometric current obtained in the presence and absence of interferent). Upon the addition of 0.2 μM MG to PBS (0.1 mM, 7.4 pH) containing 0.1 mM GSH, a well-defined amperometric current response was observed. When the interferents were injected individually to the 0.1 M PBS, the amperometric current ($I\% \leq 2.3$) nearly approached the magnitude of current detected in the absence of interferents, indicating the ability of the developed biosensor to overcome the potential interferents and its high selective nature towards MG in spite of all the other interferents. The storage stability ($\%Stability = 100 - \left[\frac{I_n - I_0}{I_0} \times 100\right]$, where I_n and I_0 are the amperometric currents measured in the 'nth' and first day) of Pt/ZnO flakes/GLO 1 bio-electrode was examined by measuring its amperometric current response to 0.2 μM MG. When the Pt/ZnO flakes/GLO 1 bio-electrode was stored in 0.1 M PBS (7.4 pH) for 18 days, no considerable decrease in the amperometric response (89% stability) to 0.2 μM MG was observed.

Quantitation of MG in grilled chicken samples

To assess the consistency of the developed biosensor, MG in grilled chicken sample was analysed using Pt/ZnO flakes/GLO 1 bio-electrode. For this study, grilled chicken was purchased from the local market and 4 g of chicken sample was homogenized with 15 mL of deionised water and centrifuged for 15 min at 8000 rpm. The 20 μL of the supernatant was added to 3 mL of PBS and amperometric studies were conducted. The unknown MG concentration in the real grilled chicken sample was calculated using the calibrated nonlinear ($I = \frac{6.62\,\mu A[MG]}{5.81\,\mu M + [MG]}$, 0.2 μM ≤ [MG] ≤ 100 μM) regression equation. Table 2 shows the results of the addition-recovery experiment using MG for five standard concentrations and the sample contained 2.52 μM concentration of MG. Then, the sample was spiked with a known concentration of MG (0.2, 0.6, 1.0, 1.5 and 2.0 μM) and the

Table 2 Results of the addition-recovery experiment using MG for five standard concentrations

Sample (4 g of grilled chicken)	MG added (μM)	Mean MG detected (μM)[a]	Recovery (%)	RSD (%) (n = 3)
1	0	2.52	–	–
2	0.2	2.76	101.5	1.05
3	0.6	3.16	101.2	0.84
4	1.0	3.49	99.3	0.49
5	1.5	4.04	100.5	0.35
6	2.0	4.54	100.5	0.35

[a]Average of three determinations

Table 3 Comparative study of existing MG biosensors with the present MG biosensor

Sample	Electrode matrix	Sensitivity ($\mu A\ \mu M^{-1}$)	Response time (s)	Recovery (%)	Biosensor efficiency (%)	LOD (nM)	Inhibition (%)	References
Human plasma	GCE/SWCNT	0.076	–	95.01–104.56	–	–	4.67	[3]
Beer/wine	GCE/Pt/SWCNT	0.114	–	95.04–104.74	–	2.80	4.21	[4]
Human blood	Pt/ZnO/GLO 1/Chitosan	0.022	–	91.15–116.488	–	–	–	[5]
Grilled chicken	Pt/ZnO/GLO 1/Chitosan	2.615	–	95.895–108.191	–	–	–	[6]
Cow milk	Pt/CeO_2/GLO 1/Chitosan	2.347	<40	98.64–102.75	–	3.65	3.21	[7]
Grilled chicken	Pt/ZnO flakes/GLO 1/Chitosan	0.281	<4	99.3–101.5	405	9	2.3	Present work

amperograms were recorded. The percentage recovery values for different concentrations of MG added, varied in the range of 99.3–101.5% and the RSD% values were within the acceptable limit (ranges from 0.35 to 1.05%). This experiment confirmed the high accuracy and good reproducibility of Pt/ZnO flakes/GLO 1 bio-electrode.

Comparison of characteristics of the present MG biosensor with the existing MG biosensor

Table 3 shows the comparative study of existing MG biosensors with the present one. Comparing with the existing MG biosensors, the present MG electrochemical biosensor showed superior performances such as higher biosensor efficiency (405%), fast response time (<4 s), excellent recovery (99.3–101.5%) and higher sensitivity (0.281 $\mu A\ \mu M^{-1}$). Moreover, it also showed that the Pt/ZnO flakes/GLO 1 bio-electrode can be further applied to detect MG in human plasma, beer and wine samples.

Conclusion

In this work, the analytical performances of MG biosensor such as biosensor efficiency and response time are reported for the first time. The GLO 1 immobilization on ZnO flakes surface was effective and didn't require any cross-linker. In the absence of the mediator, the ZnO flakes enhanced the electron transfer between GLO 1 and Pt working electrode. The immobilized GLO 1 on ZnO flakes surface retained its catalytic activity and exhibited high sensitivity. All these results showed that the Pt/ZnO flakes/GLO 1 bio-electrode was sensitive and specific for the detection of MG in grilled chicken.

Acknowledgements The authors are grateful to the Department of Science and Technology, New Delhi, for their financial support (DST/TSG/PT/2008/28, SR/FST/ETI-284/2011(C) and (Nano Mission Council (No. SR/NM/PG-16/2007)). We also acknowledge SASTRA University, Thanjavur for extending infrastructural support to carry out the study.

References

1. Singh R, Barden A, Mori T BL. Advanced glycation end-products: a review. Diabetologia. 2001;44(2): 129–146
2. Committee on Toxicity Statement on Methylglyoxal. Vol. 34, Committee on Toxicity. 2009
3. Mark AB, Poulsen MW, Andersen S, Andersen JM, Bak MJ, Ritz C, Holst JJ, Nielsen J, De Courten B, Dragsted LO, Bügel SG. Consumption of a diet low in advanced glycation end products for 4 weeks improves insulin sensitivity in overweight women. Diabetes Care. 2014;37: 88–95. https://doi.org/10.2337/dc13-0842
4. Bin L, Bihao C, Jiang S (2012) Ice-temperature storage technology of fruits and vegetables. In: Valdez B (Ed.) Food industrial processes—methods and equipment. InTech. http://www.intechopen.com/books/food-industrial-processes-methods-and-equipment/ice-temperature-storage-technology-of-fruits-and-vegetables
5. Uribarri J, Woodruff S, Goodman S, Cai W, Chen X, Pyzik R, Yong A, Striker GE, Vlassara H. Advanced Glycation End Products in Foods and a Practical Guide to Their Reduction in the Diet. J Am Diet Assoc. 2010;10(6): 911–916
6. Ansari SA, Husain Q. Potential applications of enzymes immobilized on/in nano materials: A review. Biotechnol Adv. 2012;30(3): 512–523
7. National Diabetes Fact Sheet—Centers for Disease Control and Prevention; U.S. Department of Health and Human Services. 2011;CS217080A(Division of Diabetes Translation): 1–12
8. "50 million people in India have diabetes." The Indian Express. 2012;1030869. http://archive.indianexpress.com/news/-50-million-people-in-india-have-diabetes-/1030869/
9. "Diabetes capital" tag a burden on India's heart. HindustanTimes. Lucknow; 2013. http://www.hindustantimes.com/lucknow/diabetes-capital-tag-a-burden-on-india-s-heart/story-UzEjAj4EXP2MJjTaLlIO9O.html

10. Kalousová M, Zima T, Tesař V, Dusilová-Sulková S, Škrha J. Advanced glycoxidation end products in chronic diseases—clinical chemistry and genetic background. Mutat Res Fundam Mol Mech Mutagen. 2005;579(1–2): 37–46
11. Sassolas A, Blum LJ, Leca-Bouvier BD. Immobilization strategies to develop enzymatic biosensors. Biotechnol Adv. 2012;30(3): 489–511
12. FDI General Assembly. Non-Communicable Diseases. FDI General Assembly. Hong Kong; 2012
13. Thangavel A, Alagesan S, Nesakumar N, Ramachandra BL, Gumpu MB, Vedantham S, Sethuraman S, Krishnan UM, Rayappan JBB. Optimization of Electrochemical Parameters for Specific Blood Methylglyoxal Determination Using ZnO Sepals Based Glyoxalase 1 Biosensor. Sens Lett. 2015;13(4): 328–337
14. Chatterjee S, Chen A. Voltammetric detection of the dicarbonyl compound: Methylglyoxal as a flavoring agent in wine and beer. Anal Chim Acta. 2012;751: 66–70. https://doi.org/10.1016/j.aca.2012.09.011
15. Chatterjee S, Wen J, Chen A. Electrochemical determination of methylglyoxal as a biomarker in human plasma. Biosens Bioelectron. 2013;42(1): 349–354
16. Ren X, Chen D, Meng X, Tang F, Hou X, Han D, Zhang L. Zinc oxide nanoparticles/glucose oxidase photoelectrochemical system for the fabrication of biosensor. J Colloid Interface Sci. 2009;334(2): 183–187
17. Petchthanasombat C, Tiensing T, Sunintaboon P. Synthesis of zinc oxide-encapsulated poly(methyl methacrylate)-chitosan core-shell hybrid particles and their electrochemical property. J Colloid Interface Sci. 2012;369(1): 52–57
18. Nesakumar N, Thandavan K, Sethuraman S, Krishnan UM, Rayappan JBB. An electrochemical biosensor with nanointerface for lactate detection based on lactate dehydrogenase immobilized on zinc oxide nanorods. J Colloid Interface Sci. 2014;414(xx): 90–96. https://doi.org/10.1016/j.jcis.2013.09.052
19. Singh M, Nesakumar N, Sethuraman S, Krishnan UM, Rayappan JBB. Electrochemical biosensor with ceria-polyaniline core shell nano-interface for the detection of carbonic acid in blood. J Colloid Interface Sci. 2014;425: 52–58. https://doi.org/10.1016/j.jcis.2014.03.041
20. Ezhilan M, Alagesan S, Ramachandra BL, Gumpu MB, Nesakumar N, Vedantham S, Sethuraman S, Krishnan UM, Rayappan, JBB. Chemometric Analysis for the Determination of Methylglyoxal in Grilled Chicken Using ZnO Flakes Based Glyoxalase 1 Biosensor. Sens Lett. 2015;13(3): 245–253
21. Ramachandra BL, Vedantham S, Krishnan UM, Nesakumar N, Balaguru Rayappan JB. Estimation of methylglyoxal in cow milk – an accurate electrochemical response time based approach. Anal Methods. 2016;8(10): 2207–2217. Available from: http://xlink.rsc.org/?DOI=C5AY02901E
22. Chaplen FWR. Incidence and potential implications of the toxic metabolite methylglyoxal in cell culture: a review. Cytotechnology. 1998;26(3): 173–183
23. Dem'yanets LN, Li LE, Uvarova TG. Zinc oxide: hydrothermal growth of nano- and bulk crystals and their luminescent properties. J Mater Sci. 2006;41(5): 1439–1444
24. Rodríguez-Paéz JE, Caballero AC, Villegas M, Moure C, Durán P, Fernández JF. Controlled precipitation methods: formation mechanism of ZnO nanoparticles. J Eur Ceram Soc. 2001;21(7): 925–930
25. Suchea M, Christoulakis S, Moschovis K, Katsarakis N, Kiriakidis G. ZnO transparent thin films for gas sensor applications. Thin Solid Films. 2006;515(2 SPEC. ISS.): 551–554
26. Kannan PK, Saraswathi R, Rayappan JBB. A highly sensitive humidity sensor based on DC reactive magnetron sputtered zinc oxide thin film. Sens Actuators A Phys. 2010;164(1–2): 8–14
27. Mani GK, Rayappan JBB. A highly selective room temperature ammonia sensor using spray deposited zinc oxide thin film. Sens Actuators B Chem. 2013;183: 459–466
28. Zhao Z, Lei W, Zhang X, Wang B, Jiang H. ZnO-based amperometric enzyme biosensors. Sensors. 2010;10(2): 1216–1231
29. Raoufi D, Raou D. Synthesis and microstructural properties of ZnO nanoparticles prepared by precipitation method. Renew Energy. 2013;50: 932–937
30. Arya SK, Saha S, Ramirez-Vick JE, Gupta V, Bhansali S, Singh SP. Recent advances in ZnO nanostructures and thin films for biosensor applications: Review. Anal Chim Acta. 2012;737: 1–21
31. Sivalingam D, Gopalakrishnan JB, Rayappan JBB. Structural, morphological, electrical and vapour sensing properties of Mn doped nanostructured ZnO thin films. Sens Actuators B Chem. 2012;166–167: 624–631
32. Yakimova R. ZnO materials and surface tailoring for biosensing. Front Biosci E. 2012;4(1): 254
33. Ali SMU, Ibupoto ZH, Kashif M, Hashim U, Willander M. A potentiometric indirect uric acid sensor based on ZnO nanoflakes and immobilized uricase. Sensors. 2012;12(3): 2787–2797
34. Fulati A, Ali SMU, Asif MH, Alvi NUH, Willander M, Brännmark C, Strålfors P, Börjesson SI, Elinder F, Danielsson B. An intracellular glucose biosensor based on nanoflake ZnO. Sens Actuators B Chem. 2010;150(2): 673–680
35. Bu IYY, Yang CC. High-performance ZnO nanoflake moisture sensor. Superlattices Microstruct. 2012;51(6): 745–753
36. Wahab R, Kim Y-S, Shin H-S. Synthesis, characterization and effect of pH variation on zinc oxide nanostructures. Mater Trans. 2009;50(8): 2092–2097
37. Dermenci KB, Ebin B, Gürmen S. Production of spherical Ag/ZnO nanocomposite particles for photocatalytic applications. Int J Chem Mol Nucl Mater Metall Eng. 2012;6(7): 570–572
38. Hou Z, Wang Y, Shen L, Guo H, Wang G, Li Y, Zhou S. Synthesis of dumbbell-like ZnO microcrystals via a simple solution route. Nanoscale Res Lett. 2012;7(1): 1
39. Yao L, Zheng M, Li C, Ma L, Shen W. Facile synthesis of superhydrophobic surface of ZnO nanoflakes: chemical coating and UV-induced wettability conversion. Nanoscale Res Lett. 2012;7: 216
40. Hamedani NF, Farzaneh F. Synthesis of ZnO nanocrystals with hexagonal (wurtzite) structure in water using microwave irradiation. Sci Islam Repub Iran. 2006;17(3): 231–234
41. Coates J. Interpretation of Infrared Spectra, A Practical Approach. In: Encyclopedia of Analytical Chemistry. John Wiley & Sons, Ltd; 2006
42. Scirè A, Saccucci F, Bertoli E, Cambria MT, Principato G, D'Auria S, Tanfani F. Effect of acidic phospholipids on the structural properties of recombinant cytosolic human glyoxalase II. Proteins Struct Funct Genet. 2002;48(1): 126–133
43. Liu Y, Yang Z, Du J, Yao X, Lei R, Zheng X, Liu J, Hu H, Li H. Study on the interactions of kaempferol and quercetin with intravenous immunoglobulin by fluorescence quenching, Fourier transformation infrared spectroscopy and circular dichroism spectroscopy. Chem Pharm Bull 2008;56(4): 443–451
44. Nikitina O, Shleev S, Gayda G, Demkiv O, Gonchar M, Gorton L, Csöregi E, Nistor M. Bi-enzyme biosensor based on NAD- and glutathione-dependent recombinant formaldehyde dehydrogenaseand diaphorase for formaldehyde assay. Sens Actuators B Chem. 2007;125: 1–9